PHYSICAL REVIEW B **96**, 041119(R) (2017)

Self-learning quantum Monte Carlo method in interacting fermion systems

Xiao Yan Xu,[1,2] Yang Qi,[3] Junwei Liu,[3] Liang Fu,[3] and Zi Yang Meng[1,2]
[1]*Beijing National Laboratory for Condensed Matter Physics and Institute of Physics, Chinese Academy of Sciences, Beijing 100190, China*
[2]*School of Physical Sciences, University of Chinese Academy of Sciences, Beijing 100190, China*
[3]*Department of Physics, Massachusetts Institute of Technology, Cambridge, Massachusetts 02139, USA*
(Received 15 December 2016; revised manuscript received 27 December 2016; published 18 July 2017)

The self-learning Monte Carlo method is a powerful general-purpose numerical method recently introduced to simulate many-body systems. In this work, we extend it to an interacting fermion quantum system in the framework of the widely used determinant quantum Monte Carlo. This method can generally reduce the computational complexity and moreover can greatly suppress the autocorrelation time near a critical point. This enables us to simulate an interacting fermion system on a 100×100 lattice even at the critical point and obtain critical exponents with high precision.

DOI: 10.1103/PhysRevB.96.041119

Introduction. Numerous intermetallic compounds with intriguing phenomena, such as non-Fermi liquids [1] and unconventional superconductivity [2–4] emerging from quantum critical fluctuations (antiferromagnetic [2–4], nematic [5,6], etc.), demand proper theoretical understanding. However, these systems are usually strongly correlated and can only be solved by nonperturbative methods. In the past few years, after several attempts [7–14], people have realized that determinant quantum Monte Carlo (DQMC) is one of the most suitable methods and sometimes the only available choice.

DQMC [15–17] has been widely used in the investigation of correlated fermion systems [18–32]. Despite great successes, the method also suffers from serious difficulties. In DQMC, one introduces bosonic auxiliary fields to decouple the fermion interactions[1] and then simulates the whole system by updating bosonic fields based on the corresponding weights, whose computation is very heavy since they require determinant calculations to integrate out the fermion degrees of freedom. Currently, even the fastest algorithm available still has the computational complexity in a polynomial form [33] of $O(\beta N^3)$ [34], where β is the inverse temperature and N is the system size. Even worse, this algorithm has to employ local updates and the generated configurations are usually not statistically independent, requiring long autocorrelation time. Particularly around phase transition points, the autocorrelation time becomes extremely long and also dramatically increases with the system size. Together, these severe scaling behaviors seriously limit the applications of DQMC in interacting fermion systems. For instance, in two-dimensional (2D) strongly correlated fermion systems, 24×24 is a typically accessible size.

Recently, we proposed a general-purpose method, self-learning Monte Carlo (SLMC), to speed up MC simulations [35–37]. Very encouragingly, with a highly efficient cumulative update algorithm, SLMC can generally reduce the computational complexity and dramatically decrease the autocorrelation time in fermion systems [36], yet SLMC is still an unbiased MC method without approximation. In SLMC, configurations are first updated much more cheaply according to the simple effective bosonic Hamiltonian self-learned in advance, instead of the original Fermion Hamiltonian, and heavy-duty matrix operations are greatly reduced. At the same time, the simulation is guaranteed to be statistically exact by the detailed balance principle following the original Hamiltonian deciding whether the configurations proposed by cumulative update of the effective model can be accepted.

In this Rapid Communication, we extend SLMC to fermionic quantum many-body systems in the framework of DQMC, referred to as SLDQMC. It manages to greatly reduce the computational complexity of the original DQMC, typically, by a factor of $\min\{O(\beta), O(N)\}$. Hence, as either the system sizes are larger or the temperature is lower, the speedup of SLDQMC over DQMC is greater. Moreover, in SLDQMC, the autocorrelation time is effectively reduced to $O(1)$ around phase transition points, independent of system size. With these advantages, we are able to simulate a generic 2D interacting fermion model with system size 100×100, a number unaccessible in conventional DQMC.

Basics of DQMC. To set the stage for SLDQMC, we need to first briefly introduce DQMC. Let us start with the partition function of a general fermionic quantum many-body system,

$$Z = \sum_{\{\mathcal{C}\}} \phi(\mathcal{C}) \det\left(\mathbf{1} + \mathbf{B}(\beta, 0; \mathcal{C})\right), \tag{1}$$

where $\mathcal{C} = \{s_{i,\tau}\}$ is the auxiliary field ($s_{i,\tau}$) configuration after the Hubbard-Stratonovich (HS) transformation is applied to decouple the fermion interaction terms in the Hamiltonian [17] or the bosonic filed already involved in the original model [7]. The imaginary time β is divided into M time slices ($M\Delta\tau = \beta$) and hence the configurations $\mathcal{C}$ of the bosonic fields have both spatial and temporal dependence. $\phi(\mathcal{C})$ is the bare part (including the transformation constant) of the bosonic field, and it is a scalar function. Now, for each auxiliary field configuration, the fermions are noninteracting and can hence be traced out, resulting in a determinant $\det(\mathbf{1} + \mathbf{B}(\beta, 0; \mathcal{C}))$. The matrix $\mathbf{B}(\beta, 0)$, depending on configurations $\mathcal{C}$, is a short form for the matrix product $\mathbf{B}^M \mathbf{B}^{M-1} \cdots \mathbf{B}^1$, where the matrix at time slice τ is $\mathbf{B}^\tau = \exp(\Delta\tau \mathbf{K}) \exp(\mathbf{V}(s_{i,\tau}))$, with $\mathbf{K}$

[1]In some cases [7–12], the bosonic fields already exist in the original Hamiltonian, and their fluctuations mediate effective fermion interactions.

being the tight-binding hopping matrix of the bare system in the single-particle basis and $\mathbf{V}(s_{i,\tau})$ being the fermion interaction part after HS transformation, and it describes the coupling between bosonic field and fermion bilinear [17]. The dimension of matrix $\mathbf{B}^{\tau}$ is equal to the number of degrees of freedom of fermion and scales with system size $N \sim L^d$, with L being the linear system size and d being the spatial dimension.

To update the auxiliary field configuration in DQMC, one performs local updates [15–17], i.e., by trying to flip the bosonic spins $s_{i,\tau}$ one by one through the space-time lattice βN. The acceptance ratio of such an update involves a ratio of two determinants before and after the flip. The computational complexity for evaluating a determinant is $O(N^3)$, but the local nature of the update enables one to perform a fast update with complexity $O(1)$ to calculate the ratio and complexity $O(N^2)$ to update the Green's function if the local update is accepted. However, since one needs to scan over the space-time lattice—this is called one sweep—to attempt flip the βN numbers of auxiliary field, the local update of DQMC is of computational complexity $O(\beta N^3)$.

There is another factor that further increases the computational complexity for all the Monte Carlo simulations: the autocorrelation time τ_L. In the context of DQMC, τ_L is the number of sweeps one needs to perform to have two statistically independent configurations, such that Monte Carlo measurements can be taken. Therefore, the total computational complexity in DQMC is $O(\beta N^3 \tau_L)$. At (quantum) critical points or when there are strong correlations in the auxiliary field, the autocorrelation time usually becomes very large and will scale with system size $\tau_L \sim L^z$, which is referred as critical slowing down, and z is the dynamic exponent of MC simulation. For local update, z could be very large ($\geqslant 2$). In the classical and quantum spin or bosonic systems, tailor-made global update schemes, such as the Swendsen-Wang [38], Wolff [39], and loop and directed loop [40,41], have been designed, and the dynamic exponent z can be greatly reduced. But these global update schemes are very model dependent, and in the framework of DQMC, there is still no practical global update available.

Formalism of SLDQMC. To overcome these problems, we design SLDQMC as a general-purpose solution to fermionic quantum Monte Carlo simulations. Below we describe its procedure in four steps.

At step (i), we use the local update of DQMC to generate enough configurations according to the original Hamiltonian. At step (ii), we try to obtain an effective model by self-learning [35–37]. The effective model can be very general,

$$H^{\text{eff}} = E_0 + \sum_{(i\tau);(j,\tau')} J_{i,\tau;j\tau'} s_{i,\tau} s_{j,\tau'} + \cdots, \tag{2}$$

where $J_{i,\tau;j\tau'}$s parametrizes the two-body interaction between any bosonic field in space-time. More-body interactions, denoted as $\cdots$, can also be included. In practice, we can use symmetries (rotation, translation, etc.) to reduce the number of independent interactions. We introduce a parameter γ as the range of the interactions considered in the effective model and it will be tuned to make the effective model close enough to the original model.

The training procedure is straightforward. Given a configuration $\mathcal{C}$ and corresponding weight $\omega[\mathcal{C}]$, generated in the step (i), we have

$$-\beta H^{\text{eff}}[\mathcal{C}] = \ln(\omega[\mathcal{C}]). \tag{3}$$

By combining Eqs. (2) and (3), optimized values of $\{J_{i,\tau;j\tau'}\}$ can be readily obtained through a multilinear regression [35,36] using all the configurations prepared in step (i).

At step (iii) of SLDQMC, we perform multiple local updates with H^{eff} (as in general the H^{eff} will contain a nonlocal term, which makes the cluster update difficult to implement). Unlike from the local update in DQMC [15–17], the local move of H^{eff} is very fast, as there are no matrix operations involved. Furthermore, to generate statistically independent configurations at (quantum) critical point, we need to perform about τ_L sweeps of local update. With these local updates of effective model, the configuration has been changed substantially, and we take the final configuration as a proposal for a global update for the original model. This entire process is denoted as a *cumulative update*. The acceptance ratio of the cumulative update can be derived from the detail balance as

$$A(\mathcal{C} \to \mathcal{C}') = \min\left\{1, \frac{\exp(-\beta H[\mathcal{C}'])}{\exp(-\beta H[\mathcal{C}])} \frac{\exp(-\beta H^{\text{eff}}[\mathcal{C}])}{\exp(-\beta H^{\text{eff}}[\mathcal{C}'])}\right\}. \tag{4}$$

Here one can clearly see that the closer H^{eff} is to the original Hamiltonian H with fermion integrated out, the larger $A(\mathcal{C} \to \mathcal{C}')$ becomes, and eventually, for a sufficiently good H^{eff}, $A(\mathcal{C} \to \mathcal{C}') \sim 1$ can be achieved in all practical terms (as shown below). At step (iv), following this detailed balance decision, we decide to accept or reject the final configuration. By repeating steps (iii) and (iv), we can simulate the interaction fermion systems with high efficiency.

Before we reveal the results of SLDMQC, let us discuss the enormous speedup of SLDQMC over DQMC. The complexity of the cumulative update in SLDQMC is $O(\gamma\beta N\tau_L + \beta N^2 + N^3)$ and it is comprised of two parts. First, the operation to update the effective model is $O(\gamma\beta N\tau_L)$. γ is the number of operations needed for a single local update on effective model, there are βN bosonic fields in total, and one performs τ_L sweeps on all the space-time bosonic fields. Second, the complexity of calculating the acceptance ratio in Eq. (4) is $O(\beta N^2 + N^3)$. βN^2 comes from the evaluation of matrix $\mathbf{B}(\beta,0;\mathcal{C})$, in that $\mathbf{B}(\beta,0;\mathcal{C})$ is the product of $O(\beta)$ number of $\mathbf{B}^{\tau}$ matrices, each $\mathbf{B}^{\tau}$ is a product of $O(N)$ number of sparse matrices, while the complexity of the dense and sparse matrices production here is $O(N)$. The other $O(N^3)$ comes from the complexity of calculating the determinant $\det(\mathbf{1} + \mathbf{B}(\beta,0;\mathcal{C}))$.

Comparing the $O(\gamma\beta N\tau_L + \beta N^2 + N^3)$ of SLDQMC and $O(\beta N^3\tau_L)$ of DQMC, we define a speedup factor $\mathcal{S}$ of SLDQMC over DQMC and find

$$\mathcal{S} = \min\left(\frac{N^2}{\gamma}, N\tau_L, \beta\tau_L\right). \tag{5}$$

For many models, we only need include short-range interactions in the effective model [35,36], and in this case, SLDQMC can easily reduce the computational complexity by at least $O(N\tau_L)$ or $O(\beta\tau_L)$; i.e., as the systems are larger and temperatures are lower, the SLDQMC gains more speedup. Moreover, it is clear that SLDQMC with cumulative update effectively renders the autocorrelation time for only one sweep, and hence fully cures the critical slowdown at (quantum) critical points. At last, it is worth noting that even in the worst case, where we need to take long-range interactions in H^{eff} into account, $\gamma \sim \beta N$, a large speedup, $\mathcal{S} = \mathcal{O}(N/\beta)$ can still be guaranteed; i.e., for a given temperature β, we can achieve at least $O(N)$-fold speedup. All those advantages make SLDQMC very suitable to study the interacting fermion systems with large sizes, especially around critical points.

We also note, at low temperatures, the matrix multiplication becomes numerically unstable and the commonly used stabilization algorithm scales with $O(\beta N^3)$, which would dominate the complexity of multiplication itself. However, even in this case, SLDQMC still offers the speedup discussed above by overcoming the critical slowdown. Attempts to improve the algorithm of stabilization is in progress.

Results. To demonstrate the power of SLDQMC, we consider an interacting fermion model with ferromagnetic transverse-field Ising spins coupled to a Fermi surface. The Hamiltonian is comprised of three parts,

$$H = H_f + H_s + H_{sf}. \tag{6}$$

The fermion part, $H_f = -t\sum_{\langle ij\rangle\lambda\sigma}(c^\dagger_{i\lambda\sigma}c_{j\lambda\sigma} + \text{H.c.}) - \mu\sum_{i\lambda\sigma} n_{i\lambda\sigma}$, describes spin-1/2 fermion hoppings on a bilayer ($\lambda = 1,2$) square lattice, with intralayer hopping t and chemical potential μ. The Ising spin part is $H_s = -J\sum_{\langle ij\rangle} s^z_i s^z_j - h\sum_i s^x_i$, with ferromagnetic J and transverse field h introducing (quantum) fluctuations to the system. At $T = 0$, the Ising spins go though a quantum phase transition from ferromagnetic (FM) phase to paramagnetic (PM) phase at $h_c/J = 3.04$ with $(2+1)$d Ising universality [10,42,43], and at finite temperature, the transition from FM to PM is of 2d Ising universality. The $H_{sf} = -\xi\sum_i s^z_i(\sigma^z_{i1} - \sigma^z_{i2})$ is the coupling between Ising spin and fermion spin, and the coupling favors a parallel (antiparallel) alignment of Ising spin and fermion spin in layer 1 (2). Such bilayer setup guarantees a sign-problem-free QMC simulation in the framework of DQMC [10].

Once switching on the coupling, $\xi = 1$, the fluctuations in the Ising spins introduce effective interaction to the fermions, and the fermions will in turn introduce long-range interactions among the Ising spins. Our model in Eq. (6) thus provides an ideal situation to study the behavior of itinerant electrons with quantum fluctuations in the vicinity of (quantum) critical points in a controlled manner. The itinerant quantum critical point (FM-QCP in this case), Fermi-liquid instabilities at magnetic quantum phase transition [44,45], and its applications to heavy-fermion materials and transition-metal alloys (cuprates and pnictides) are of vital importance and broad interest to the condensed-matter physics community.

Theoretical approaches able to address the quantum phase transition of the model in Eq. (6) and the properties of the quantum critical region are still under intensive development [46–51]. Recent numerical evidence shows the universality is different from both the $(2+1)$d Ising as well as Hertz-Millis-Moriya predictions, and non-Fermi liquid is being observed in the quantum critical region [14].

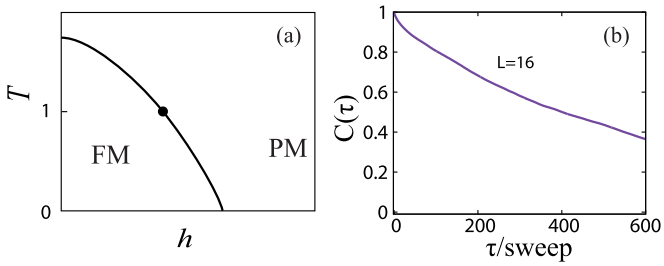

FIG. 1. (a) Schematic phase diagram of the transverse-field Ising model coupled to Fermi surface. As a function of the transverse field, the system (both fermions and Ising spins) goes through a transition from ferromagnetic (FM) metal to paramagnetic (PM) metal. The black dot is the finite-temperature critical point [$T = 1, h_c = 2.774(1)$] where we systematically demonstrate the superior performance of SLDQMC over DQMC. (b) Autocorrelation function $C(\tau)$ for $L = 16$ system at the critical point in panel (a), for local update with DQMC, where the autocorrelation time is very long (larger than 600 sweeps). The autocorrelation function is defined as $C(\tau) = (\langle M(0)M(\tau)\rangle - \langle M\rangle^2)/(\langle M^2\rangle - \langle M\rangle^2)$ with $M(\tau)$ being the total magnetization of Ising spins for the τth sweep.

Although the quantum critical properties are complicated, finite-temperature FM to PM phase transition is relative simple and one can have a simple schematic phase diagram as shown in Fig. 1(a). In this work, we demonstrate the power of SLDQMC by focusing on FM-PM critical point at a finite temperature: $\beta = 1.0$, $\Delta\tau = 0.05$, $M = 20$, and $h_c = 2.774(1)$, as the black dot in Fig. 1(a). At the critical point, configurations of Ising spins generated by local updates become strongly correlated, as shown by the autocorrelation function of Ising spin in Fig. 1(b) for $L = 16$, and it is the exact manifestation of critical slowdown.

To train the effective model in Eq. (2), we use $1 - \mathcal{R}^2 = \langle(H^{\text{eff}} - H)^2\rangle/(\langle H^2\rangle - \langle H\rangle^2)$, where $\mathcal{R}^2$ is the coefficient of determination (as a figure of merit "score") for the multilinear regression in Eq. (3). Figure 2 shows the $1 - \mathcal{R}^2$ of the multilinear regression as we vary the range of interactions in the effective model. For the purple line in Fig. 2, we fix the $J_{i,\tau;j,\tau}$ to only nearest neighbor in the spatial direction and explore the range of the interaction in the temporal direction. It turns out that the interaction in the temporal direction is long ranged, and since we choose $M = 20$ time slices in total, one needs to consider the interaction up to $M = 10$. The spatial range of interaction, on the other hand, is short ranged. As shown with green line in the Fig. 2, we keep the interaction in the temporal direction to $M = 10$ and plot of $1 - \mathcal{R}^2$ as a function of spatial range; one can clearly see that after the second nearest neighbor, $1 - \mathcal{R}^2$ is already converged to a very small value. In the real fitting, when let the range of interactions in both temporal and spatial directions is free, we find for an $L = 8$ system at $\beta = 1.0$, in total 16 $J_{i,\tau;j,\tau'}s$ (two spatial neighbors, ten temporal neighbors, four spatial-temporal neighbors) in H^{eff} are needed to give the best

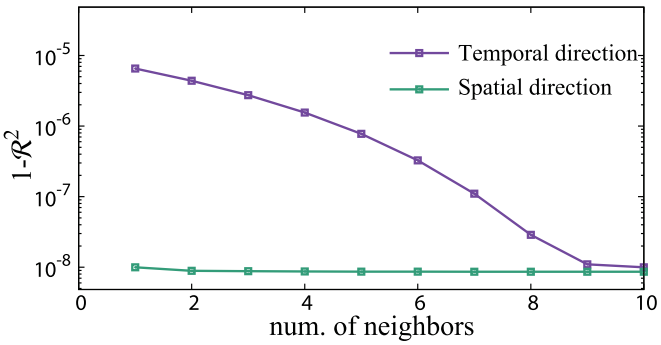

FIG. 2. The coefficient of determination for multilinear regression $\mathcal{R}^2$ decides how many $J_{i,\tau;j,\tau'}$s (how many neighbor interactions) need to be considered in the H^{eff}. Purple line shows the $1-\mathcal{R}^2$ for the temporal neighbors while fixing the spatial neighbor nearest. Green line shows the $1-\mathcal{R}^2$ for the spatial neighbors while fixing the temporal neighbors. The temporal interaction is more long ranged (up to the tenth nearest neighbor) but the spatial interaction is short ranged (up to the second nearest neighbor).

fit at the critical point. We have used 10^5 configurations in the fitting.

With effective model obtained from $L=8$, we now perform SLDQMC with cumulative update for larger system sizes. The great improvement is shown in Fig. 3. The autocorrelation time of DQMC presents the typical critical slowdown behavior: $\tau_L \propto L^z$ with $z=2.1(1)$. However, SLDQMC overcomes such a slowdown completely: τ_L is a constant as small as one for all the system sizes simulated, and the dynamic exponent of SLDQMC with cumulative update is practically $z=0$. Because of such superior behavior of SLDQMC, a speedup of $\mathcal{S}=O(N)$ for our 2d system is easily achieved, as promised in the discussion of Eq. (5). We want to note although a completely mathematical rigorous proof is lacking here, the observed constant autocorrelation is a direct evidence of rapid convergence of our method.

With such a speedup by SLDQMC, we are now able to access an enormously large system. In Fig. 4, we measure the uniform Ising spin susceptibility $\chi(L)=\frac{1}{L^2}\sum_{ij}\int_0^\beta d\tau\langle s^z_{i,\tau}s^z_{j,0}\rangle$.

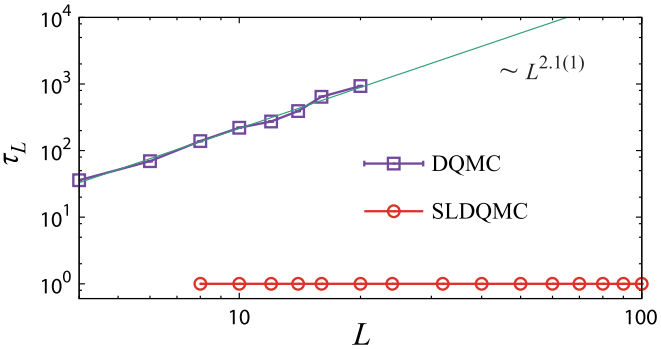

FIG. 3. Comparison of τ_L between DQMC and SLDQMC at the critical point. For DQMC, the critical slowdown with $\tau_L \sim L^{2.1(1)}$ is observed, while for SLDQMC, the critical slowdown has been complete cured, $\tau_L=1$, for all the system sizes up to $L=100$.

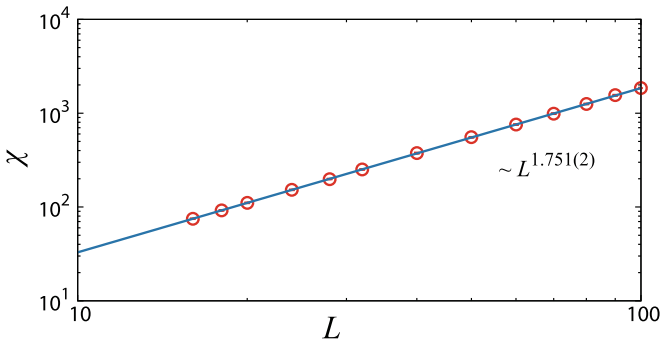

FIG. 4. Uniform spin susceptibilities χ at the critical point as a function of system sizes, $\chi \propto L^{2-\eta}$ with $\eta=\frac{1}{4}$ as the anomalous dimension of 2d Ising universality. The linear system size is as large as $L=100$.

Since the system is at a 2d Ising critical point, $\chi(L)\propto L^{2-\eta}$, with $d=2$ and $\eta=\frac{1}{4}$. We are able to simulate systems as large as $L=100$, and $\chi \propto L^{2-\eta}$ is clearly seen with $2-\eta=1.751(2)$.

Conclusions. In this Rapid Communication, we extended the SLMC method [35,36] to the fermionic quantum many-body systems and implemented it in the framework of DQMC. The obtained SLDQMC, with cumulative update scheme, provides a general-purpose solution to fermionic quantum Monte Carlo simulations. We demonstrate that SLDQMC can greatly reduce the autocorrelation time and speed up the simulation at least of $O(N)$-fold at the critical point. To illustrate the strength of SLDQMC, a 2D interacting fermion system with size as 100×100 is able to be simulated. We believe SLDQMC opens a promising avenue for the numerical investigation of interacting fermionic systems. After three decades of intensive studies with DQMC, it is now possible to simulate system sizes as large as those in the QMC study of quantum spin systems. Many standing problems in the interacting fermion system are now resolved with SLDQMC. For example, very recently, an application of SLDQMC on the itinerant quantum criticality with both frustration and non-Fermi-liquid behaviors has become available [52].

Acknowledgments. X.Y.X. and Z.Y.M. acknowledge the support from the Ministry of Science and Technology of China under Grant No. 2016YFA0300502, the National Natural Science Foundation of China under Grants No. 11421092, No. 11574359, and No. 11674370, and the National Thousand-Young Talents Program of China. The work at MIT is supported by the DOE Office of Basic Energy Sciences, Division of Materials Sciences and Engineering, under Award No. DE-SC0010526. L.F. is partly supported by the David and Lucile Packard Foundation. We thank the following institutions for allocation of CPU time: the Center for Quantum Simulation Sciences in the Institute of Physics, Chinese Academy of Sciences, the National Supercomputer Center in Tianjin (http://nscc-tj.gov.cn), and the Gauss Centre for Supercomputing e.V. (http://www.gauss-centre.eu) for providing access to the GCS Supercomputer SuperMUC at Leibniz Supercomputing Centre (LRZ, http://www.lrz.de).

[1] H. v. Löehneysen, J. Phys.: Condens. Matter **8**, 9689 (1996).
[2] T. Park, F. Ronning, H. Q. Yuan, M. B. Salamon, R. Movshovich, J. L. Sarrao, and J. D. Thompson, Nature (London) **440**, 65 (2006).
[3] T. Helm, M. V. Kartsovnik, I. Sheikin, M. Bartkowiak, F. Wolff-Fabris, N. Bittner, W. Biberacher, M. Lambacher, A. Erb, J. Wosnitza, and R. Gross, Phys. Rev. Lett. **105**, 247002 (2010).
[4] K. Hashimoto, K. Cho, T. Shibauchi, S. Kasahara, Y. Mizukami, R. Katsumata, Y. Tsuruhara, T. Terashima, H. Ikeda, M. A. Tanatar, H. Kitano, N. Salovich, R. W. Giannetta, P. Walmsley, A. Carrington, R. Prozorov, and Y. Matsuda, Science **336**, 1554 (2012).
[5] Z. Liu, Y. Gu, W. Zhang, D. Gong, W. Zhang, T. Xie, X. Lu, X. Ma, X. Zhang, R. Zhang, J. Zhu, C. Ren, L. Shan, X. Qiu, P. Dai, Y.-f. Yang, H. Luo, and S. Li, Phys. Rev. Lett. **117**, 157002 (2016).
[6] W. Zhang, J. T. Park, X. Lu, Y. Wei, X. Ma, L. Hao, P. Dai, Z. Y. Meng, Y.-f. Yang, H. Luo, and S. Li, Phys. Rev. Lett. **117**, 227003 (2016).
[7] E. Berg, M. A. Metlitski, and S. Sachdev, Science **338**, 1606 (2012).
[8] Y. Schattner, S. Lederer, S. A. Kivelson, and E. Berg, Phys. Rev. X **6**, 031028 (2016).
[9] F. F. Assaad and T. Grover, Phys. Rev. X **6**, 041049 (2016).
[10] X. Y. Xu, K. S. D. Beach, K. Sun, F. F. Assaad, and Z. Y. Meng, Phys. Rev. B **95**, 085110 (2017).
[11] Y. Schattner, M. H. Gerlach, S. Trebst, and E. Berg, Phys. Rev. Lett. **117**, 097002 (2016).
[12] S. Gazit, M. Randeria, and A. Vishwanath, Nat. Phys. **13**, 484 (2017).
[13] Z.-X. Li, F. Wang, H. Yao, and D.-H. Lee, Sci. Bull. **61**, 925 (2016).
[14] X. Y. Xu, K. Sun, Y. Schattner, E. Berg, and Z. Y. Meng, arXiv:1612.06075.
[15] R. Blankenbecler, D. J. Scalapino, and R. L. Sugar, Phys. Rev. D **24**, 2278 (1981).
[16] J. E. Hirsch, Phys. Rev. B **31**, 4403 (1985).
[17] F. Assaad and H. Evertz, in *Computational Many-Particle Physics*, Lecture Notes in Physics Vol. 739, edited by H. Fehske, R. Schneider, and A. Weiße (Springer, Berlin, 2008), pp. 277–356.
[18] J. E. Hirsch, Phys. Rev. B **28**, 4059 (1983).
[19] R. Preuss, A. Muramatsu, W. von der Linden, P. Dieterich, F. F. Assaad, and W. Hanke, Phys. Rev. Lett. **73**, 732 (1994).
[20] F. F. Assaad, M. Imada, and D. J. Scalapino, Phys. Rev. Lett. **77**, 4592 (1996).
[21] M. Brunner, F. F. Assaad, and A. Muramatsu, Phys. Rev. B **62**, 15480 (2000).
[22] R. Staudt, M. Dzierzawa, and A. Muramatsu, Eur. Phys. J. B **17**, 411 (2000).
[23] C. N. Varney, C.-R. Lee, Z. J. Bai, S. Chiesa, M. Jarrell, and R. T. Scalettar, Phys. Rev. B **80**, 075116 (2009).
[24] Z. Y. Meng, T. C. Lang, S. Wessel, F. F. Assaad, and A. Muramatsu, Nature (London) **464**, 847 (2010).
[25] F. Parisen Toldin, M. Hohenadler, F. F. Assaad, and I. F. Herbut, Phys. Rev. B **91**, 165108 (2015).
[26] Y. Otsuka, S. Yunoki, and S. Sorella, Phys. Rev. X **6**, 011029 (2016).
[27] M. Hohenadler, Z. Y. Meng, T. C. Lang, S. Wessel, A. Muramatsu, and F. F. Assaad, Phys. Rev. B **85**, 115132 (2012).
[28] F. F. Assaad, M. Bercx, and M. Hohenadler, Phys. Rev. X **3**, 011015 (2013).
[29] Z. Y. Meng, H.-H. Hung, and T. C. Lang, Mod. Phys. Lett. B **28**, 1430001 (2014).
[30] Y.-Y. He, H.-Q. Wu, Y.-Z. You, C. Xu, Z. Y. Meng, and Z.-Y. Lu, Phys. Rev. B **93**, 115150 (2016).
[31] H.-Q. Wu, Y.-Y. He, Y.-Z. You, T. Yoshida, N. Kawakami, C. Xu, Z. Y. Meng, and Z.-Y. Lu, Phys. Rev. B **94**, 165121 (2016).
[32] Y.-Y. He, H.-Q. Wu, Y.-Z. You, C. Xu, Z. Y. Meng, and Z.-Y. Lu, Phys. Rev. B **94**, 241111 (2016).
[33] M. Jerrum and A. Sinclair, SIAM J. Comput. **22**, 1087 (1993).
[34] E. Loh, J. Gubernatis, R. Scalettar, S. White, D. Scalapino, and R. Sugar, Int. J. Mod. Phys. C **16**, 1319 (2005).
[35] J. Liu, Y. Qi, Z. Y. Meng, and L. Fu, Phys. Rev. B **95**, 041101 (2017).
[36] J. Liu, H. Shen, Y. Qi, Z. Y. Meng, and L. Fu, Phys. Rev. B **95**, 241104 (2017).
[37] Y. Nagai, H. Shen, Y. Qi, J. Liu, and L. Fu, arXiv:1705.06724.
[38] R. H. Swendsen and J.-S. Wang, Phys. Rev. Lett. **58**, 86 (1987).
[39] U. Wolff, Phys. Rev. Lett. **62**, 361 (1989).
[40] H. G. Evertz, Adv. Phys. **52**, 1 (2003).
[41] O. F. Syljuåsen and A. W. Sandvik, Phys. Rev. E **66**, 046701 (2002).
[42] P. Pfeuty and R. J. Elliott, J. Phys. C **4**, 2370 (1971).
[43] G. G. Batrouni and R. T. Scalettar, *Ultracold Gases and Quantum Information*, Lecture Notes of the Les Houches Summer School in Singapore Vol. 91 (Oxford University Press, Oxford, UK, 2011).
[44] G. R. Stewart, Rev. Mod. Phys. **73**, 797 (2001).
[45] H. v. Löhneysen, A. Rosch, M. Vojta, and P. Wölfle, Rev. Mod. Phys. **79**, 1015 (2007).
[46] A. V. Chubukov, C. Pépin, and J. Rech, Phys. Rev. Lett. **92**, 147003 (2004).
[47] A. V. Chubukov and D. L. Maslov, Phys. Rev. Lett. **103**, 216401 (2009).
[48] T. Senthil, Phys. Rev. B **78**, 035103 (2008).
[49] S.-S. Lee, Phys. Rev. B **80**, 165102 (2009).
[50] D. Dalidovich and S.-S. Lee, Phys. Rev. B **88**, 245106 (2013).
[51] A. L. Fitzpatrick, S. Kachru, J. Kaplan, and S. Raghu, Phys. Rev. B **89**, 165114 (2014).
[52] Z. H. Liu, X. Y. Xu, Y. Qi, K. Sun, and Z. Y. Meng, arXiv:1706.10004.